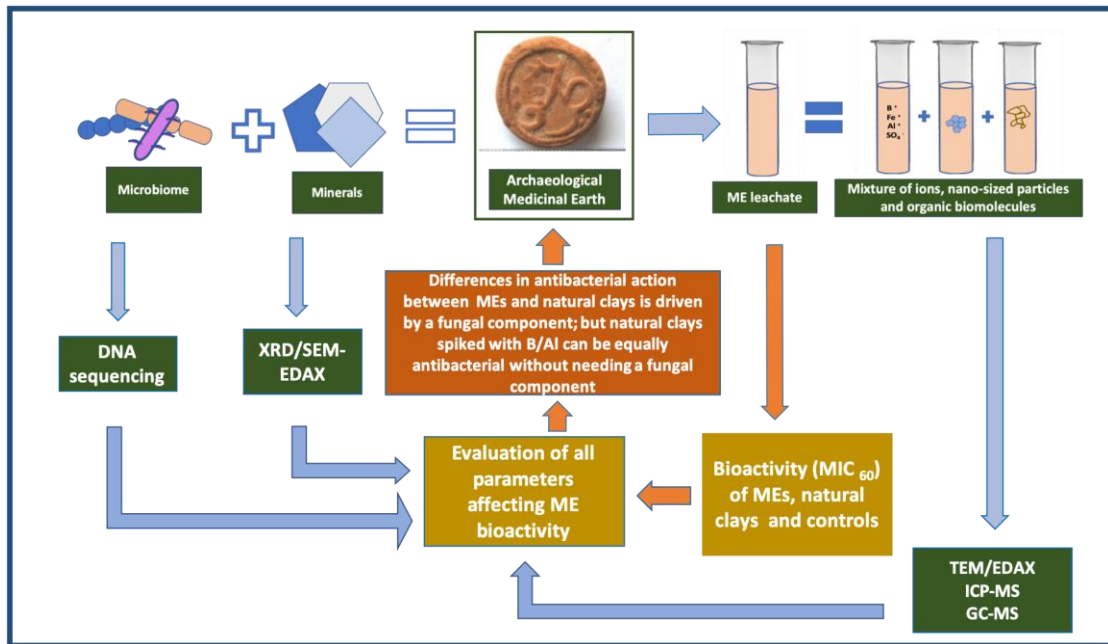


1
2
3

Graphical abstract



4
5
6
7
8
9
10
11
12
13
14
15
16
17
18
19
20
21
22
23
24
25
26
27
28
29

30 **The interweaving roles of mineral and microbiome**
31 **in shaping the antibacterial activity of archaeological medicinal clays**

32
33
34 G.E. Christidis ¹, C.W. Knapp ² D. Venieri ³, I. Gounaki ³, C. Elgy ⁴,
35 E. Valsami-Jones ⁴, E. Photos-Jones ^{5,6*}

36
37 *effie.photos-jones@glasgow.ac.uk

38
39 1. School of Mineral Resources Engineering, Technical University of Crete, 73100 Chania,
40 Greece

41 2. Civil and Environmental Engineering, University of Strathclyde, Glasgow G1 1XQ, UK

42 3. School of Environmental Engineering Technical University of Crete, 73100 Chania, Greece

43 4. School of Geography, Earth and Environmental Sciences, University of Birmingham,
44 Edgbaston, Birmingham B15 2TT, UK

45 5. Analytical Services for Art and Archaeology (Ltd), Glasgow G12 8JD, UK

46 6. Archaeology, School of Humanities, University of Glasgow, Glasgow G12 8QQ, UK

47
48
49 **Abstract**

50 **Ethnopharmacological relevance:** Medicinal Earths (MEs), natural aluminosilicate-
51 based substances (largely kaolinite and montmorillonite), have been part of the
52 European *pharmacopoeia* for well over two millennia; they were used generically as
53 ‘antidotes to poison’

54 **Aim of the study:** To test the antibacterial activity of three Lemnian and three
55 Silesian Earths, medicinal earths in the collection of the Pharmacy Museum of the
56 University of Basel, dating to 16th-18th century and following a prescribed
57 methodology (see graphical abstract). To assess and prioritize the parameters which
58 drive their antibacterial activity, if present.

59 **Materials and Methods:** The medicinal earths are characterised chemically (ICP-MS),
60 mineralogically (both bulk (XRD) and at the nano-sized level (TEM-EDAX)); their
61 organic load (bacterial and fungal) is DNA-sequenced; their bioactivity (MIC₆₀) is
62 tested against Gram-positive, *S. aureus* and Gram-negative, *P. aeruginosa*. The
63 bioactivities (MIC₆₀) of natural clays from Lemnos, N Aegean, and Melos, SW Aegean,
64 spiked with Al, Fe, Ti, and B are also tested against the same pathogens for purposes
65 of comparison, as well as controls.

66 **Results.** Not all MEs are antibacterial. Of the three Lemnian Earths, only two are
67 antibacterial against both pathogens; of the Silesian Earths only one is mildly
68 antibacterial and against Gram-negative pathogen, only. The bioactivity of the two
69 Lemnian Earths is driven by a fungal component, *Talaromyces spp*, a fungus of the
70 family of *Trichocomaceae* (order Eurotiales), historically associated with *Penicillium*.
71 This fungus was not found in the natural Lemnos clays examined here. Comparable
72 bioactivity with that of the two Lemnian Earths can be obtained from
73 kaolinitic/smectitic clays spiked with B or Al. Interestingly controls displayed similar
74 behaviour.

75 **Conclusions.** It is not known whether archaeological medicinal earths were used as
76 antibacterials, over and above as absorbants of toxins. Nevertheless, in the absence of
77 spiking elements like B and Al, some display antibacterial properties which appear to
78 have their origins in an organic (fungal) load. This observation necessitates the
79 investigation of the origin and function of the fungal component in MEs.

80

81 **Keywords:** medicinal earths, Lemnian, Silesian, bioactivity, *Talaromyces spp*, mineral,
82 nanoparticle, antimicrobial resistance

83 *1.Introduction*

84 Medicinal Earths (MEs) have been part of the European *pharmacopoeia* for well over
85 two millennia. Stamped medicinal earths or *terra sigillata* are natural aluminosilicate-
86 based substances (largely kaolinite and montmorillonite) with a well-recorded history
87 of use as ‘antidotes to poison’ and spanning over two and a half millennia (Macgregor,
88 2013). Stamping the earth with a readily identifiable seal conferred confidence on the
89 product but also provided control of the trade in such substances from antiquity to
90 modern times (Nutton 2004). Lemnian Earth (LE), from the island of Lemnos, N.E.
91 Aegean, was the oldest and most established and with continuous use until the early
92 20th century (Hasluck, 1910; Sealy, 1919). It is reported, amongst others, in
93 Theophrastus (4th c BC), Dioscorides (1st c AD) and Pliny (2nd c AD). Galen (2nd c AD)
94 visited the island and gave a detailed account of the various stages in the process of
95 extraction and ‘washing’ thereof, both activities purported to have taken place once a
96 year (Brock 1929, 185). Sometime in Late Antiquity and early Byzantine times the
97 practice appears to have waned or stopped completely but it was certainly revived in
98 the Ottoman period when its extraction and distribution was tightly regulated (Hasluck
99 and Hasluck, 1929; Tourptsoglou-Stephanidou, 1986). As a result, many new MEs
100 began to appear in the markets across the Mediterranean, Northern Europe and the
101 Middle East aiming to emulate (and rival) LE’s widely acknowledged beneficial
102 properties. Most carried the same tradition of being stamped, hence their generic name,
103 *terra sigillata*.

104 In the 16th c the most prominent medicinal earth emerging out of Central Europe was
105 Terra Silesia, in present day SW Poland (Dannenfeldt,1984). It was also a *terra*
106 *sigillata* since it bore the coat of arms of the city of Striga (Strigovia, Striegau, or
107 Strzegom) consisting of three mountain peaks (see Fig. 1f). Terra Silesia acquired quite
108 a reputation with doctors following the Paracelsus school who attributed its healing
109 properties to the gold within the local auriferous granite. Medicinal earths from varying
110 localities survive to this day in a number of museum collections as collectors’
111 curiosities (Duffin, 2013). Only very few have been subjected to analysis (Hardy and
112 Rollinson 2016).

113 Over many years we have carried out research into some of the minerals discussed in
114 the Greco-Roman technical and medical texts, from the perspective of geo-
115 archaeological work and in an attempt to locate them in the field (Photos-Jones and
116 Hall, 2011; Photos-Jones et al., 2015, 2016). We have suggested reasons why LE would
117 have been efficacious, based on sampling of local sedimentary clays from the purported
118 area of its extraction (Kotsinas, N.E. Lemnos) (Hall and Photos-Jones, 2008). Recently
119 we have analysed three samples of Lemnos *terra sigillata* (we will refer to them as
120 Lemnian Earth) in the collection of the Pharmacy Museum of the University of Basel
121 (Fig. 1a-c) and qualitatively assessed their antibacterial activity (Photos-Jones et al.,
122 2017).

123 This paper revisits the same three samples of Lemnian Earth (Fig. 1a-c: 700.4, 700.17,
124 700.18) in an attempt to assess the same activity, quantitatively, (MIC₆₀), against two
125 pathogens (Gram-negative *P. aeruginosa* and Gram-positive *S. aureus*). These specific
126 bacterial strains were chosen because of their relation to public health issues, and their

127 use as valuable bacterial indicators. Further, it compares their efficacies as
128 antibacterials with a contemporary set of Silesian Earths (Fig. 1d-f 703.1, 703.2, 703.3),
129 also dating to 16th-18th century AD. Although all six MEs were purported to be
130 medicinal, only two were found to be demonstrably antibacterial, and against both of
131 the above pathogens. Suffice it to say that clays can still be considered ‘medicinal’ even
132 though they might display no antibacterial action. Antibacterial action is a property that
133 we are interested in because it is easily measurable and quantifiable. We therefore asked
134 the question: which parameters drive differences in antibacterial action between
135 different samples of medicinal earths? Is it their mineralogy, at both bulk and nanosized
136 level? or is it their elemental composition? or is it other factors?

137
138 By other factors we refer to the MEs’, natural or acquired organic load, their bacterial
139 and fungal microbiome. This microbial load never leaves the clay because the latter is
140 never heated, at any stage of its preparation as a ‘medicine’. Bacteria and fungi,
141 naturally present within soils, can potentially have the inadvertent effect of rendering
142 the clays medicinal (as antioxidants, antibacterials or metal chelators) on account of
143 their production of secondary metabolites (e.g., Keller, 2019; Pettit, 2011). This is the
144 result of either intra- and inter-specific interactions (Tyc et al., 2016), or toxicological
145 conditions, the presence of metals (Locatelli et al., 2016) or salts (Medina et al., 2015).
146 It can also be the result of their growth conditions. Ecologically, the production of
147 secondary metabolites is advantageous to the microorganism since it increases its
148 competitiveness or survival in the environment (Macheleidt et al., 2016).

149
150 We therefore propose a step-by-step investigation of the MEs, from the perspective of
151 bulk mineralogy, chemistry of the leachate, and nanoparticle characterization, followed
152 by DNA sequencing of their microbiome, and MIC₆₀ testing, against specific pathogens
153 in order to shed light into the contribution of individual components to the MEs’
154 bioactivity. The graphical abstract at the start of the paper illustrates our proposed
155 method which consists of the undertaking of a number of analytical techniques aimed
156 to evaluate: a. the bulk mineral (XRD); b. the mineral leachate (TEM/EDAX/ICP-MS);
157 c. the organic constituent (DNA sequencing of biome/GC-MS of secondary
158 metabolites); d. the testing of bioactivity against select pathogens. In this study we have
159 not undertaken the investigation of secondary metabolites (via GC-MS) but refer to
160 them in previous work (Photos-Jones et al., 2017).

161
162 Having outlined our approach, (graphical abstract), we shall demonstrate that some
163 clay samples can be rendered antibacterial on account of specific elements and/or
164 nanosized particles, while others, with similar mineralogy, can be rendered antibacterial
165 on account of their microbiome, bacterial or other. Demonstrating the idea that there
166 might be multiple drivers to antibacterial activity within the same type of clay could
167 potentially have far reaching implications.

168
169 Resistance against effective antibiotics has emerged as a serious and growing
170 phenomenon in contemporary medicine, making the growth inhibition of virulent
171 pathogens for humans and the environment quite a challenge (Manaia et al., 2016;
172 Venieri et al., 2017a, 2017b). Clays have the potential to exhibit bactericidal effect in
173 both Gram-negative and Gram-positive strains through the exchange of components
174 between them and bacteria and the ultimate prevention of the latter’s metabolic
175 functions (Haydel et al., 2008). Clay nanoparticles- based techniques have already been
176 introduced to induce antibacterial action within aquatic environments and during water

177 treatment (Unuabonah and Taubert, 2014). Although bacteria are considered very
178 adaptive to hostile conditions, up until now no resistance mechanism similar to that
179 against antibiotics has been recorded in clays (i.e. induction of antibiotic resistance
180 genes).

181

182 Archaeological medicinal earths are clay-based and have an uninterrupted history of
183 use (in the case of LE) of over two millennia. It is not clear whether they were intended
184 as antibacterials, and not merely as absorbants of toxins. Nevertheless, with this paper
185 and the one preceding it (Photos-Jones et al., 2017) we have demonstrated that some
186 *can* be antibacterial. What we seek to understand is the parameters driving this
187 antibacterial behaviour in a small number of archaeological medicinal clays.

188

189 **INSERT FIG. 1**

190



Fig. 1a 700.4
Lemnian Earth
Mus. No 01432

Fig. 1b 700.17
Lemnian Earth
Mus. No 01422

Fig. 1c 700.18
Lemnian Earth
Mus. No 01424

Fig. 1d 703.1
Terra Silesia
Mus. No 01114

Fig. 1e 703.2
Terra Silesia
Mus. No 01133

Fig. 1f 703.3
Terra Silesia.
Mus. No 01137

191

192 *2. Materials and Methods*

193

194 *2.1 Materials*

195 A total of eighteen samples were examined in this study; they fall into three groups:

196 a. six MEs consisting of three from Lemnos (LEs) (700.4, 700.17 and 700.18) and three
197 from Silesia (SEs) (703.1, 703.2, 703.3). This group of samples derive, as mentioned
198 earlier, from the collection of the Museum of Pharmacy, University of Basel (museum
199 accession numbers are given in Fig. 1).

200 b. four natural clays consisting of two from Lemnos, N.E. Aegean (700.19 and 700.20)
201 from the area of Kotsinas, NE Lemnos, the purported area of extraction of LE and
202 another two from Melos, S.W. Cyclades. The Melos bentonite sample (933) originates
203 from the Angeria mine, N.W. Melos, and the Melos kaolin sample (900.9). from the
204 abandoned kaolin mine at Loulos, 2 km north of the Paleochori Bay, S.E. Melos. The
205 Melos samples are introduced here as ‘good’ basic clays with which to build synthetics.

206 c. eight synthetic samples prepared from Melos bentonite and kaolin and spiked with
207 four different elements (i.e. Ti, Al, Fe, and B). These include Melos smectite and
208 kaolinite treated with aluminum sulfate ($\text{Al}_2(\text{SO}_4)_3 \cdot 16\text{H}_2\text{O}$), (samples 6 and 7
209 respectively); smectite and kaolinite treated with boric acid (H_3BO_3) (samples 4 and 5,
210 respectively); smectite and kaolinite treated with natural fine iron oxides collected from
211 the island of Kea, N Cyclades, (Photos-Jones et al., 2018)(samples 14 and 15,
212 respectively); and finally, smectite and kaolinite treated with analytical grade TiO_2
213 (anatase, Merck) (samples 10 and 9 respectively). The Kea samples have been chosen
214 on account of the purity/finesse of their iron oxides and their recorded use from the 4th
215 c BC.

216 The synthetic aluminium sulfate- and boron- treated samples were prepared as follows.
217 1g of clay (kaolin or bentonite) were placed in 50ml polyethylene centrifuge tubes. 15
218 ml of 1N H₃BO₃ or 0.5 N Al₂(SO₄)₃ (both of Sigma Aldrich analytical grade) solution
219 were added, the clays were dispersed in an ultrasonic probe for 20s, and the tubes were
220 covered with a stopper and left overnight. Subsequently, the suspensions were
221 centrifuged, the clear supernatant solutions were decanted and the whole procedure was
222 repeated. In the following day the suspensions were centrifuged and the tubes with the
223 clay were dried at 60°C and the dry clay powders were transferred in glass vials and
224 stored. The synthetic samples with addition of iron oxides and TiO₂ were prepared by
225 adding 0.1 g to 0.4 g of bentonite or kaolin. The materials were ground with an agate
226 pestle and mortar using acetone to obtain fine grained homogeneous mixtures.

227

228 2.2 Methods

229 2.2.1 Mineralogy - XRD

230 The mineralogical composition of all samples was determined with X-ray diffraction
231 (XRD), at the School of Mineral Resources Engineering, Technical University of Crete,
232 on a Bruker D8 Advance Diffractometer equipped with a Lynx Eye strip silicon
233 detector, using Ni-filtered CuK α radiation (35 kV, 35mA). Data were collected in the
234 2 θ range 3-70° 2 θ with a step size of 0.02° and counting time 1 s per strip step (total
235 time 63.6 s per step). The XRD traces were analyzed and interpreted with the Diffrac
236 Plus software package from Bruker and the Powder Diffraction Files (PDF). The
237 quantitative analysis was performed on random powder samples (side loading
238 mounting) by the Rietveld method using the BMGN code (Autoquan© software
239 package version 2.8).

240

241 2.2.2 Bioactivity testing

242 2.2.2.1 Bacterial strains and antimicrobial tests

243 The bacterial indicators used for the assessment of antimicrobial properties of the
244 samples were *Pseudomonas aeruginosa* NCTC 10662 (Gram-negative) and
245 *Staphylococcus aureus* NCTC 12493 (Gram-positive). Both bacteria were cultured on
246 LB agar (LABM) and LB broth (LABM) and the desired bacterial concentration in each
247 experimental run was adjusted based on the McFarland scale, according to which, an
248 inoculum absorbance of 0.132 measured at 600 nm corresponds approximately to a cell
249 density of

250 1.5×10^8 CFU/mL

251 . Our goal in this study was to employ both a Gram-negative and a Gram-positive
252 species, considering their structural differences and physiology, which impose adverse
253 behaviour in stressed environmental conditions. Both bacteria are often reported for
254 their notable antibiotic resistance and their adaptability in hostile surroundings (Swetha
255 et al. 2010; Venieri et al. 2017b).

256

257 2.2.2.2 Sample preparation and antimicrobial tests

258 The antibacterial activity of the samples was assessed over both bacterial indicators
259 using their aqueous leachates. All leachates were prepared at a concentration of 600
260 mg/mL, mixing samples with sterile deionized water, followed by ultrasonication
261 (Julabo ultrasonic bath) for 30 min at 25 °C and centrifugation at 10000 g for 15 min to
262 remove all solids from the solution. The leachate was decanted, sterilized in the
263 autoclave (20 min, 120 °C), and tested against bacteria.

264

265 In order to compare the difference in activity of samples with and without organic
266 content, chemical oxidation was performed to breakdown organic matter with sodium
267 hypochlorite (NaOCl) as the oxidizing agent (Anderson, 1963). An aliquot 4 mL of a
268 NaOCl (6%) solution was mixed with of 2g of each sample into a centrifuge tube, which
269 was then placed in a boiling water bath for 15 min. Then, the sample was centrifuged
270 at 800 g for 10 min and the solution was decanted. The procedure was repeated 3 times,
271 after which the solid was washed with sterilized water, dried and processed for further
272 biological analysis. For reference to this protocol, see Andrews (2001).

273

274 Antimicrobial activity of all samples (prior to and post chemical oxidation) was studied
275 using the broth microdilution method and estimating the Minimum Inhibitory
276 Concentration that inactivated 60% of the bacterial population (MIC₆₀). MICs were
277 measured labeling 96-well sterile microtiter trays with dilutions of each sample. The
278 bacterial inoculum in each case was adjusted to 10⁵ CFU/mL. Microtiter trays were
279 incubated at 37°C for 18-24 h, followed by optical density measurement at 630 nm,
280 using a microplate reader (Labtech LT-4000 Plate Reader) and Manta LML software.

281

282

283 *2.2.3 Chemical analyses of leachates-ICP-MS*

284 The aqueous leachates were produced by adding 0.2 g of the samples in 5 ml distilled
285 water, dispersing with ultrasonic probe for 20 s, allowing standing for 1 h and
286 subsequent centrifugation. The supernatant was stored in polyethylene bottles for ICP-
287 MS analysis (7500CX coupled with Autosampler Series 3000, both by Agilent
288 Technologies) for major and trace elements. The precision of the analyses was tested
289 using elemental standards (1000mg/L) by Merck . The relative standard deviation of
290 the analyses varied according to the concentration, typically 7% for the major elements,
291 less for the trace elements.

292

293

294 *2.2.4 TEM-EDAX*

295 For Transmission Electron Microscopy (TEM) with EDAX approximately 10mg of
296 powder were suspended in 10ml of ultrapure water. The suspension was vortexed for 1
297 minute at full power (Rotamixer Hook and Tucker Ltd.) The sample was processed in
298 the ultrasonic bath for 5 minutes (Branson 1510 ultrasonic bath) and centrifuged in
299 15ml tubes in the Eppendorf centrifuge 5804R, at 4,000rpm for 10 minutes for clay
300 samples, and at 2,500rpm for 11 minutes for iron oxide samples, to remove particles
301 above 450nm. A drop of 35 microliters of the supernatant was deposited onto 200mesh
302 copper grids with carbon film and left there without drying for one hour. The excess
303 sample was wicked from the grid, and the grid was washed 4x in water to remove any
304 salts. The grid was dried for 16 hours before use. TEM images and EDX measurements
305 were performed by the Birmingham University Centre for Electron Microscopy, using
306 a Jeol 2100 microscope.

307

308 *2.2.5 Particle size analysis*

309 Particle size for the samples were measured by DLS using a Malvern Instruments
310 Zetasizer nano ZS with a red (366 nm) laser. A method was developed to remove the
311 larger particles and provide stable suspensions of the smaller particles for DLS analysis.
312 The powders were dispersed in a 0.2% suspension of Novachem surfactant (Postnova

313 Analytics UK Ltd.) in ultrapure water. The suspension was shaken thoroughly, vortexed
314 (Rotamixer, Hook and Tucker Ltd.) at full power for 30 s and treated in the ultrasonic
315 bath (Branson, 1510) for 5 min. The samples were centrifuged at 3000 rpm, for 5 min
316 in 15 ml tubes using an Eppendorf 5804R centrifuge. This removed the larger particles
317 from the samples. Stable suspensions were obtained under these conditions.

318 The zeta potential measurements of these suspensions were negative, and between -40
319 and -50 mV, due to the effect of the Novachem surfactant which produced a high
320 surface charge. It follows that the zeta potential was altered and so is not representative
321 of the original material. However, this enabled us to stabilise the suspensions and
322 allowed reproducible size measurements to be made for the smallest particulate size
323 fraction.

324 2.2.6 DNA sequencing

325 DNA were extracted using MoBio PowerSoil Extraction kits (Qiagen) according to
326 manufacturer's procedures, except sample materials were agitated using a FastPrep24
327 cell homogenizer (MP Biomedicals; 6.0 speed, 2 x 20 seconds). Additionally, samples
328 were initially incubated at 70C for 10 minutes to facilitate the DNA extraction from
329 Gram-positive microorganisms.

330

331 Purity and quantity of extracted DNA were measured using UV-micro-
332 spectrophotometry. Extracts are stored at -80°C and further handled under UV-
333 irradiated biological cabinets with HEPA-filter laminar-flow air flow. Samples were
334 routinely diluted 1:50 with molecular-grade water to minimize inhibitors and improve
335 reaction efficiency of downstream processes.

336

337 Polymerase chain reaction (PCR) was used to selectively target the hypervariable V4
338 region of the 16S-rRNA gene. Primers were forward (AYTGGGYDTAAAGNG;
339 position 563-577) and combined set of reverse (TACNVGGGTATCTAATCC,
340 TACCRGGGTHCTAATCC, TACCAGAGTATCTAATTC, and
341 CTACDSRGGTMTCTAATC; position 907-924). To minimize cost, primers were
342 further 'bar-coded' with a short 8-base genetic sequence to allow multiple samples to
343 be simultaneously sequenced and sorted post-analytically using RDP initial pipeline
344 bioinformatics tool (Cole et al., 2014;
345 <http://pyro.cme.msu.edu/><<https://mail.campus.gla.ac.uk/owa/redir.aspx?C=QAAlSmAq6PZR-ZWaTX0sUwu9AOPrSgI-UF8DmdH3dbzOhsDWft3UCA..&URL=http%3a%2f%2fpyro.cme.msu.edu%2f>>).

348

349 The presence of fungal and chloroplast DNA were tested by PCR with primers targeting
350 the 18S-rRNA gene (Hadziavdic et al., 2014) and 16S-rRNA gene of chloroplasts, using
351 aforementioned bacterial forward primer (position 563-577) and the CYAN-786-a
352 probe modified to become a reverse primer (Knapp and Graham, 2004), respectively.

353

354 Subsequent analysis found previous universal primers for detecting fungus failed to
355 detect members *Talaromyces spp.* As such, additional de novo primers were designed
356 (in this study) for the detection of *Talaromyces sp.* (via intergenic spacer region) based
357 on Genbank accession (JN899375) using NCBI's Primer-BLAST online design tool:
358 TTGAGGGCAGAAATGACGCT (forward, 5'-3') and
359 TGAAGAACGCAGCGAAATGC (reverse, 5'-3'). In silico analysis of primer
360 specificity via BLASTn predict detection of *Talaromyces spp.* and *Penicillium spp.*,

361 both of the Trichocomaceae family of Eurotiales order.

362

363 Each 100µL PCR reaction mixture consisted of 10µL of diluted DNA sample, 50µL
364 Taq PCR Master Mix kit (Qiagen; consisting of 1.5 mM MgCl₂, 2.5 units of Taq DNA
365 polymerase, 1x proprietary PCR buffer, and 200 mM of each dNTP), 10µL 10x-primer
366 mixture (0.2µM final concentration of each primer). Reaction conditions were as
367 follows, on a BioRad iCycler5 (BioRad, Hercules, CA USA) instrument: 3-min initial
368 denaturation (94°C); 30 cycles of: denaturation (30s at 94°C), primer annealing (30s at
369 temperatures specific for each assay: 58°C for 16S-rRNA and chloroplast, and 60°C for
370 *Talaromyces*), and product extension (1 min at 72°C); and a final extension (10 min at
371 72°C). When completed, the instrument maintained the samples at 8°C.

372

373 To remove excess primers and un-polymerised nucleotides for bacterial DNA
374 sequencing, PCR product were purified using QiaQuick PCR Purification kit (Qiagen).
375 Quantities of PCR product were quantified by UV micro-spectrophotometrically,
376 combined, and condensed to 30mL, > 20 ng/mL. Library preparation (e.g., adapter
377 ligation) and MiSeq high-throughput sequencing (Illumina) were conducted by GATC-
378 Biotech (Konstanz, Germany) with full quality-control and quality-assurance. The
379 number of MiSeq reads per sample varied. Phylogenetic identity of each sequence was
380 determined based on alignments with the “Classifier” function (Wang et al., 2007) of
381 the RDPpipeline, which maintains databases for 16S- (and 18S-) rRNA sequences
382 (Cole et al., 2014). The bootstrap cut-off was predetermined to be 70% based on
383 sequence length.

384

385 3. Results

386 3.1 The mineralogy of MEs and natural clays

387 Table 1 shows the results of XRD analysis of six MEs and the four natural clays from
388 Melos and Lemnos. LE 700.4 and 700.17 consist of kaolinite, illite and quartz, with
389 dolomite being the dominant phase in 700.4 and hematite being a minor phase in
390 700.17. 700.18 consists of smectite, quartz, illite and albite. The Silesian Earths (SEs)
391 are primarily kaolinite with illite with varying amounts of quartz and small quantities
392 of anatase. Melos 900.9 and 933 are natural kaolinitic and smectitic clays respectively,
393 while chlorite and alunite are present in natural Lemnos clays (700.19 and 700.20).
394 Varying amounts of iron oxide are present in the three red samples (703.2, 700.17,
395 700.19). Reference samples SWy-2 and KGa-2 re smectite and kaolin rich respectively
396 GIORGO WHO IS THE SUPPLIER OF THESE CLAYS. PLS INSERT.

397

398 **INSERT TABLE 1**

399 **Table 1** XRD analyses of Silesian and Lemnian Earths; also, geological samples from
400 Kotsinas, Lemnos, 700.19 and 700.20 and geological samples from Melos 933 and
401 900.9 (see discussion) included here for purposes of comparison; n.d. = not detected.
402 Samples with asterisk (700.4, 700.17, 700.18, 700.19 and 700.20) were first published
403 by Photos-Jones et al (2017). Also reference samples SWy-2 and KGa-2.

404

	703.1	703.2	703.3	700.4*	700.17*	700.18*	700.19*	700.20*	933	900.9	Swy-2	KGa-2
Mineralogical Composition	Terra Silesia	Terra Silesia	Terra Silesia	Terra Lemnia (after Photos-Jones et al 2017)*	Terra Lemnia (after Photos-Jones et al 2017)*	Terra Lemnia (after Photos-Jones et al 2017)*	Natural red clay from Kotsinas, Lemnos	Natural clay from Kotsinas, Lemnos	natural smectite (Melos)	natural Kaolin (Melos)	natural smectite Wyoming	natural kaolin Georgia
Dolomite	n.d.	n.d.	n.d.	65.2	n.d.	n.d.	n.d.	n.d.	n.d.	n.d.	n.d.	n.d.
Kaolinite	31.2	87.9	67.4	17.3	37.4	n.d.	69.3	1	6.3	48.6	n.d.	97.6
Smectite/montmorillonite	n.d.	n.d.	n.d.	n.d.	n.d.	66	n.d.	35.1	71.7	n.d.	78.5	n.d.
Quartz	32.8	n.d.	25.8	7.6	17.7	6.9	n.d.	21	0.2	28.9	10.5	traces
Opai-CT/ cristoballite	n.d.	n.d.	n.d.	n.d.	n.d.	n.d.	4.5	n.d.	n.d.	5.9	n.d.	n.d.
Illite	28.1	n.d.	6.5	9.9	41	18.1	n.d.	13.3	n.d.	n.d.	n.d.	n.d.
Anatase	1.2	4.6	0.3	n.d.	n.d.	n.d.	n.d.	n.d.	1.3	0.1	n.d.	2.4
Albite	n.d.	n.d.	n.d.	n.d.	n.d.	9	n.d.	12.7	n.d.	n.d.	n.d.	n.d.
Alunite	n.d.	n.d.	n.d.	n.d.	n.d.	n.d.	22.5	n.d.	n.d.	3.3	n.d.	n.d.
Biotite	n.d.	n.d.	n.d.	n.d.	n.d.	n.d.	n.d.	n.d.	n.d.	n.d.	0.6	n.d.
Calcite	n.d.	n.d.	n.d.	n.d.	n.d.	n.d.	n.d.	8.1	5.2	n.d.	1.2	n.d.
Chlorite	n.d.	n.d.	n.d.	n.d.	n.d.	n.d.	n.d.	8.9	n.d.	n.d.	1.5	n.d.
Halite	n.d.	n.d.	n.d.	n.d.	n.d.	n.d.	n.d.	n.d.	n.d.	6.2	n.d.	n.d.
Hematite	n.d.	7.5	n.d.	n.d.	3.8	n.d.	1.8	n.d.	n.d.	n.d.	n.d.	n.d.
K-Feldspar	6.7	n.d.	n.d.	n.d.	n.d.	n.d.	n.d.	n.d.	14.8	n.d.	5.2	n.d.
Natroalunite	n.d.	n.d.	n.d.	n.d.	n.d.	n.d.	n.d.	n.d.	n.d.	7	n.d.	n.d.
Pyrite	n.d.	n.d.	n.d.	n.d.	n.d.	n.d.	n.d.	n.d.	0.5	n.d.	n.d.	n.d.
Tridymite	n.d.	n.d.	n.d.	n.d.	n.d.	n.d.	1.9	n.d.	n.d.	n.d.	n.d.	n.d.
Plagioclase	n.d.	n.d.	n.d.	n.d.	n.d.	n.d.	n.d.	n.d.	n.d.	n.d.	1.7	4.6
Gypsum	n.d.	n.d.	n.d.	n.d.	n.d.	n.d.	n.d.	n.d.	n.d.	n.d.	traces	n.d.

405
406
407
408
409
410
411

In summary, the six archaeological and the four natural clay samples are broadly classified as either kaolinitic (700.17, all SEs, 700.19 and 900.9) or as smectitic (700.18, 700.20 and 933). 700.4 is primarily dolomitic with some kaolinite. In the section that follows we proceed to establish which of the above are bioactive.

412 3.2. Antibacterial activity of MEs, natural and synthetic clays

413

414 We first investigate the antibacterial activity of the six archaeological samples and the
415 two Lemnos natural clays (700.19, 700.20) (Fig. 2 and Suppl files 1a and 1b). The
416 MIC₆₀ of the LEs is significantly lower than the MIC₆₀ of the SEs. The ranges of
417 MIC₆₀ values of LE were 50-90 mg/mL and 12.5-45 mg/mL for *P. aeruginosa* and *S.*
418 *aureus*, respectively, with the leachate of 700.17 being more active than the others.
419 The respective MIC₆₀ values for SE were 66-264 mg/mL for *P. aeruginosa* and 132
420 mg/mL for *S. aureus*, respectively. The order of bioactivity of the original samples
421 towards the Gram-negative *P. aeruginosa* is 700.17 and 700.18 > 703.1 > 700.4 >
422 703.2 > 703.3; The order of bioactivity of samples towards the Gram-positive *S.*
423 *aureus* is 700.17 > 700.18 > 700.4 > all 703 series samples. However, the aqueous
424 leachates of 703.1; 703.2 and 703.3 can hardly be described as “antimicrobial”,
425 because the obtained MIC₆₀ values were considerably over 50 natural mg/mL. Natural
426 clay samples 700.19 and 700.20 show low to no bioactivity. A sample of natural near
427 pure alunogen (Al₂(SO₄)₃·17H₂O) from the solfatara at Fyriplaka, SE Melos (sample
428 3), displayed here for purposes of comparison, is the most bioactive.

429

430 In summary, only two LEs (700.17, 700.18) are bioactive; 700.4, a dolomitic clay with
431 small amounts of kaolinite, is not bioactive against *P. aeruginosa*. Lemnos natural clays
432 700.19, 700.20 and all the SEs (703.1, 703.2 and 703.3) are not bioactive following the
433 criteria implemented here (MIC₆₀ < 50mg/ml). Given that kaolinite-rich clays can be
434 both bioactive (700.17) and non-bioactive (700.19, 703.2) we suggest that mineralogy
435 is not a key factor driving bioactivity. The same conclusion applies for the smectitic
436 clays (bioactive: 700.18; non-bioactive 700.20).

437

438 Turning now to the bioactivity of the synthetic samples (Suppl file 1a and Fig. 2), Melos
439 smectite + B (sample 4) and kaolinite + B (sample 5) are the most effective synthetics

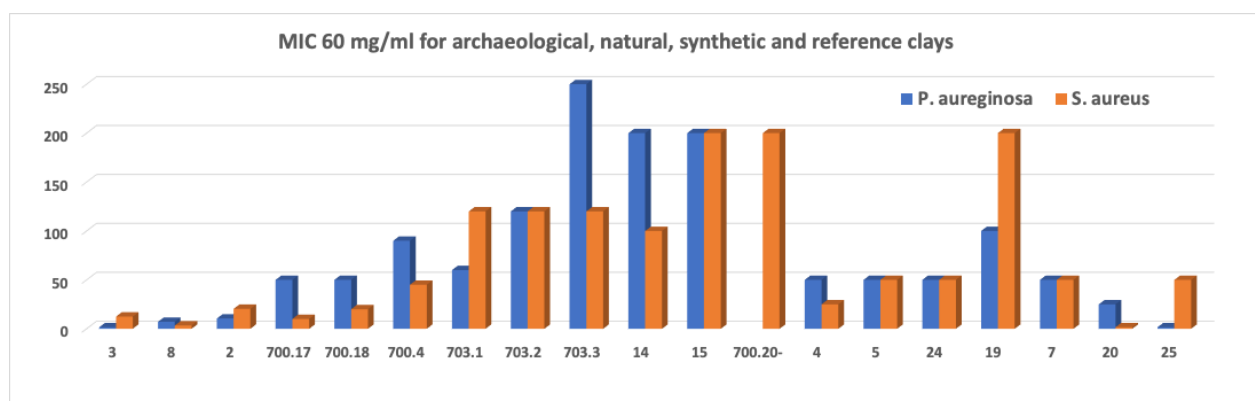
440 against both *P. aeruginosa* and against *S. aureus*, with (4) being better than (5) re the
 441 latter. Melos kaolinite + Al (7) is equally effective. Melos smectite + Fe (15) and Melos
 442 kaolinite + Fe (14) are not bioactive against either Gram-negative and Gram-positive
 443 bacteria. Melos smectite + Ti (10) and kaolinite + Ti (9) are also non-active and neither
 444 is Al-spiked Melos smectite (6). Solutions of reagent-grade boric acid (2) and reagent
 445 grade aluminium sulphate (8) are also included here for comparison. As already
 446 mentioned the most effective antibacterial is sample 3, natural alunogen, from SE
 447 Melos, which is not a clay.

448

449 Finally, we turn now to the two reference clays, kaolinite-rich (KGa-2)(sample 16)
 450 and smectite-rich SWy-2 (sample 21). They have each been tested as antibacterials and
 451 are shown to be non-active (see Suppl file 1a). Further to that, they have each been
 452 spiked with the same four elements discussed here and tested under the same conditions
 453 as above: (KGa-2 + Fe)(sample 17), (KGa-2 + Ti)(sample 18), (SWy-2 + Fe)(sample
 454 22) and (SWy-2 + Ti)(sample 23) are all non-active. Instead only (SWy-2 + B) (sample
 455 24), (SWy-2 + Al)(sample 25) (KGa-2 + B)(sample 19), and (KGa-2 + Al)(sample 20),
 456 were found to be active and against both Gram-positive and Gram-negative bacteria
 457 (see Fig. 2)

458

459



460

461

462

463 Fig. 2 Illustration of relative bioactivity between archaeological MEs, natural (700.19,
 464 700.20) synthetic samples as well as reference samples consisting of
 465 kaolinitic/smectitic clays spiked with Al, B, Ti and Fe. Only samples showing
 466 bioactivity are displayed. Blue denotes *P. aeruginosa* and Red *S. aureus*.

467

468 In summary, the most active clay samples against *both* pathogens are the two LEs,
 469 700.17, 700.18, as well as the two boron-rich Melos synthetic samples (4 and 5) and
 470 the aluminium-rich Melos kaolinite (7). Equally strong is the response of the reference
 471 clay samples (20, 24, 25) also including B and Al. As for clays spiked with Ti (9 and
 472 10) or Fe (14 or 15) they were inactive. Similarly for the two reference samples. What
 473 transpires from the above results is that:

- 474 a. smectitic clays can be *both* bioactive (700.18) *and* non bioactive (700.20).
 475 Equally, kaolinitic clays can be *both* bioactive (700.17) *and* non bioactive
 476 (700.19).
- 477 b. Reference (N. American clays) whether smectites or kaolins are not, *on their*
 478 *own*, antibacterial. Both Melos and reference clays become antibacterial when
 479 spiked with B and Al

480 c. It follows that bulk mineralogy does *not* drive bioactivity but addition of certain
481 chemical elements, like B and Al, does.

482

483 Referring back to the graphical abstract, the next step is to investigate in detail the
484 chemical make-up of the leachate of the bioactive MEs and synthetics and the range of
485 trace elements associated with each group. Suffice it to say that the graphical abstract
486 has no prescribed sequence in the analysis. It is the combined results from all techniques
487 and how one feeds into the other that help shape our understanding of the antibacterial
488 efficacy of these clays.

489

490 3.2. The chemical composition of the leachates of the bioactive MEs

491

492 Table 2 compares the chemical composition of the leachates of the six MEs, the two
493 natural clays from Lemnos (700.19 and 700.20) and the two from Melos (900.9 and
494 933) and three synthetics (4, 5 and 7). The range of parameters appears at first
495 bewildering and comparisons on an element by element basis seems to confuse rather
496 simplify the picture.

497

498 The chemical composition of the six archaeological MEs, the four naturals (700.19,
499 700.20, 900.9 and 933) and the bioactive synthetics (4, 5 and 7) is shown in Table 2.
500 Focusing on the three bioactive synthetic samples above and the two bioactive
501 archaeological LEs (700.17 and 700.18) we show that 700.17 is more abundant in Al,
502 Ti, V, Cr, Cu, Sr and Ba than, for example 900.9. The latter is deficient in Al and thus
503 it is not expected to be bioactive. It is only with enhanced amounts of (spiking with) B
504 and Al that Melos kaolinite can match the bioactivity of archaeological LE 700.17. On
505 the other hand, comparison of smectitic LE 700.18 with the natural Melos smectite 933,
506 suggests that this latter clay cannot be bioactive, either, unless spiked with Al given
507 the small concentrations in that element as well as, Ti, V, Cr and Cu. Regarding the
508 natural Lemnos clays, 700.19 and 700.20, although rich in Ti, V, Mn and Ba, it has
509 been demonstrated that they are not bioactive (Fig. 2).

510

511 Turning now to the SEs, the B content (in ppb) in the leachates is higher than that of
512 the LEs and yet the SE with the highest boron (703.2) is not antibacterial. In the case
513 of 703.1, the Al content of the leachate is very low and yet this particular ME is
514 antibacterial (against *P. aeruginosa*). Ti concentration is the highest in 703.2 and
515 700.19 and yet none of these two samples are bioactive. Interestingly sample 703.2, the
516 richest in iron oxide (Table 1) has a very low Fe content in the leachate, compared to
517 700.17 and 700.18. Finally, Melos smectite spiked with Al (6) is non-bioactive despite
518 having similar or near-similar Al contents as the bioactive MEs. This may be due to the
519 fact that Al is precipitated due to the buffering capacity of smectite.

520

521 In summary, there is no obvious correlation between elemental composition of the
522 leachate and bioactivity, and in reference to the elements investigated in detail here,
523 namely Ti, Al, B, Fe. Samples with the above elements, whether MEs, naturals or
524 synthetics, can be *either* bioactive or non-bioactive.

525

526 **INSERT TABLE 2**

527 **Table 2** ICP-MS data for the leachates of MEs, natural Lemnos clays (700.19 and
528 700.20) and synthetic clays (4, 5, 7): bdl= below detection ; adl= above detection limit.
529 Concentraions of the major elements (Si, Al, Mg, Fe, Ca, Na and K) are in ppm. The
530 remaining elements are in ppb.
531

	703.1	703.2	703.3	700.4	700.17	700.18	4	5	7	900.9	933	700.19	700.20
Na	6	6	6	1	2	3	adl	9	5	adl	17	nd	nd
Mg	12	2	4	59	1	10	22	14	3	22	1	nd	nd
Al	2	24	2	4	4	4	28	33	adl	0	1	nd	nd
Si	2	11	1	1	2	1	1	3	bdl	1	7	nd	nd
K	10	5	3	2	9	4	13	8	1	14	3	nd	nd
Ca	8	4	7	89	3	6	7	532	5	8	2	nd	nd
Fe	1	1	0	1	18	14	0	5	0	6	0	nd	nd
Li	40	42	20	33	24	2	4	18	7	1	8	6	76
B	35	52	14	7	16	12	bdl	6	2	35	20	5	12
Ti	41	1260	448	115	216	827	1	47	5	1	48	1478	485
V	bdl	8	2	26	51	71	bdl	bdl	bdl	bdl	3	95	49
Cr	2	1	1	13	38	7	bdl	bdl	4	bdl	1	32	62
Mn	1099	72	14	43	65	258	4	2	27	5	bdl	979	291
Co	3	1	0	bdl	1	4	bdl	2	bdl	bdl	bdl	14	9
Ni	34	38	14	bdl	4	9	4	19	24	5	9	13	82
Cu	15	18	20	176	17	31	8	2	15	8	7	28	14
Zn	324	543	119	3	14	29	26	83	452	36	6	34	35
As	bdl	bdl	12	3	77	5	bdl	bdl	bdl	bdl	bdl	5	0
Se	bdl	bdl	bdl	bdl	bdl	bdl	bdl	bdl	bdl	bdl	18	nd	nd
Rb	5	8	5	16	52	25	4	103	1	4	8	29	38
Sr	32	51	45	323	52	25	209	706	32	214	10	301	92
Y	1	bdl	1	bdl	bdl	bdl	bdl	1	bdl	bdl	bdl	nd	nd
Mo	4	6	2	bdl	bdl	bdl	4	2	1	4	1	nd	nd
Cd	bdl	bdl	bdl	bdl	bdl	bdl	bdl	bdl	bdl	bdl	bdl	nd	nd
Sn	bdl	bdl	bdl	bdl	bdl	bdl	bdl	bdl	bdl	bdl	bdl	nd	nd
Sb	2	2	2	bdl	bdl	bdl	0	2	2	0	bdl	nd	nd
Cs	5	11	6	2	12	4	4	22	3	4	5	1	2
Ba	31	27	60	53	136	629	71	13	51	73	bdl	865	78
Hg	11	10	0	bdl	bdl	bdl	bdl	bdl	bdl	bdl	bdl	nd	nd
Pb	bdl	1	7	17	10	40	7	bdl	0	7	1	33	8
U	0	0	0	bdl	bdl	bdl	8	3	0	0	0	nd	nd

532

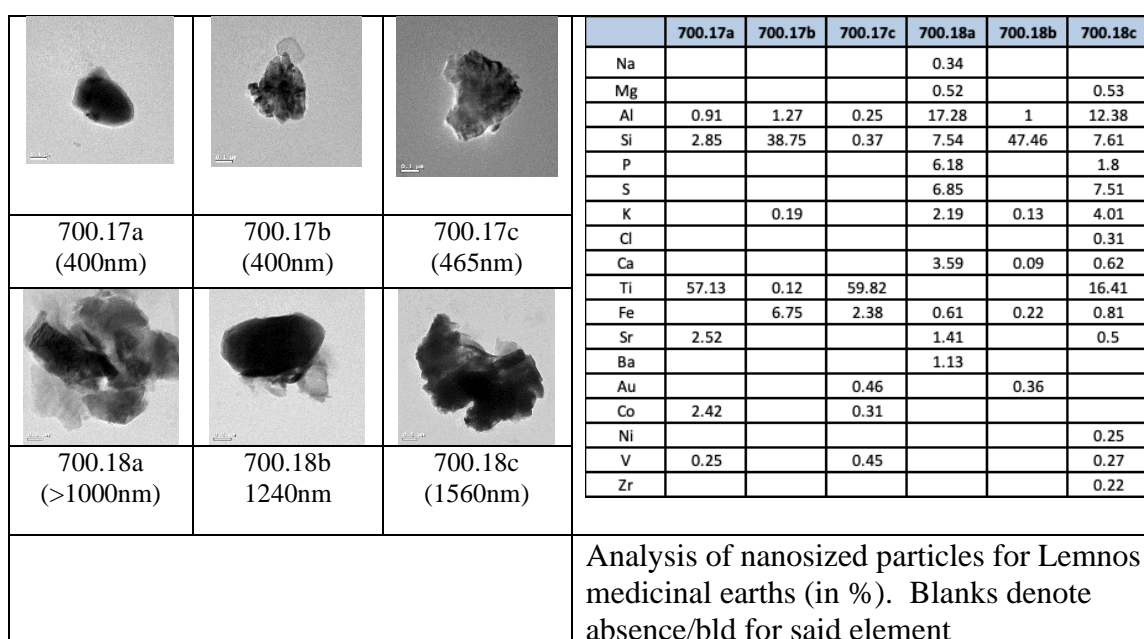
533 3.5. Nanoparticle analysis

534 TEM/EDX data of the fine fractions of the bioactive samples (700.17, 700.18) are
535 shown in Fig. 3. For the rest of the non-bioactive samples see and suppl files 2a-b. The
536 particles of 700.17a and c are characterized by the presence of anatase (TiO₂
537 polymorph) even though it was not detected in the bulk sample (Table 1). The analysis
538 of 700.17b is consistent with silicates and clays containing Fe and low levels of titanium
539 oxide, and may represent a mixture of phases. The cobalt and vanadium present are
540 also seen in the ICP-MS data (Table 2) and may be associated with titanium oxide
541 minerals.

542
543
544
545

INSERT FIG. 3

Fig. 3 Nanoparticles of bioactive LEs



546
547
548
549
550
551
552
553
554
555
556
557

The particles from 700.18 are of three different compositions: the analysis of particle 700.18c is consistent with a mixture of clay minerals and anatase, with cobalt and vanadium being present. The XRD analysis (Table 1) did not show any anatase in the bulk material, but the leachate showed high Ti levels (Table 2). In contrast, the composition of 700.18b is consistent with the presence of quartz and illite/mica and low levels of clay minerals, in line with the XRD data for the bulk material (Table 1). The composition of 700.18a is variable, with a wide range of elements present. The levels of phosphorous and sulfur may indicate some organic material. There also appears to be clay minerals present. Suppl files 2 show TEM images and EDAX table of data for the non-bioactive samples, whether MEs (SEs) or naturals (Lemnos natural clays).

558
559
560

In summary, the nanosized fractions of 700.17 and 700.18 reflect their bulk compositions, but they are not informative of the difference in bioactivity between these two samples and the non-bioactive samples.

561
562
563
564
565
566
567

Regarding the particle size analysis data, the average diameters of the two archaeological samples is 200nm (700.17) and 309nm (700.18) (see suppl file 2b); their large standard deviations indicate highly variable particle sizes. The size variation in these samples is attributed to the coexistence of clay and non-clay mineral nanoparticles (quartz, anatase, carbonates, Fe-oxyhydroxides) which are expected to have different sizes.

568
569
570

3.6. The organic load: DNA community analysis

571
572
573
574

The quantities of extracted DNA from all samples were relatively low (< 2ng/ul), or < 1.0 ng/ul, of starting material (Table 3); for example, 703.2 and 703.3 yielded 1.2 and

575 1.5 ng/ul, of DNA material, respectively. Although these values fell below the range
 576 for quantification (i.e. [DNA] are not significantly greater than zero), bacterial signals
 577 were noticed following PCR amplifications. Similar PCR screens, using
 578 cyanobacterial/chloroplast 16S-rRNA gene-specific primers and presumed universal
 579 primers for fungus (Hadziavdic et al., 2014), did not reveal any strong signals (except
 580 trace chlorophyll/chloroplast in 700.18). As such, metataxonomic analysis of the
 581 microbial communities initially focused on the bacteria. The results are presented in
 582 Table 3 and in more detail in Suppl file 3.

583

584 **INSERT TABLE 3**

585

586 **Table 3** Bacteria identified from DNA extracted from four samples, based on 16S-
 587 rRNA meta-taxonomic analysis; their relative abundances are denoted, as % of total.
 588 Superscripts refer to the bacterial genus present within each sample.

589

Bacterial phylum	700.17 ¹	700.18 ²	700.19 ³	703.1 ⁴	Genus
α -proteobacteria	44.6	55.8	0	30	<i>Bradyrhizobium</i> ^{1,2} , <i>Sphingomonas</i> ¹ , <i>Acidiphilum</i> ⁴ , <i>Brevundimonas</i> ¹ , <i>Devosia</i> ¹ , <i>Microvirga</i> ⁴
β -proteobacteria	41.7	4.7	0	0	<i>Achromobacter</i> ¹ , <i>Comamonas</i> ²
γ -proteobacteria	4.4	2.3	5	0	<i>Acinetbacter</i> ¹ , <i>Pseudomonas</i> ² , <i>Aeromonas</i> ³
ϵ -proteobacteria	0	2.3	0	0	<i>Acrobacter</i> ²
Actinobacteria	0	2.3	0	0	<i>Gaiella</i> ²
Bacteroidetes	2.2	18.6	0	0	<i>Flavobacterium</i> ^{1,2}
Chlorobi	0	0	15	0	<i>Chlorobium</i> ³
Chloroflexi	0.7	0	5	0	<i>Anaerolinea</i> ^{1,3}
Cyanobacterium	0	2.3	0	0	<i>GpXIII</i> ²
Firmicutes	0	2.3	5	0	<i>Staphylococcus</i> ² , <i>Clostridium</i> ³
Fusobacteria	0	0	5	0	<i>Fusobacteria</i> ³
Thermotogae	2.2	0	10	0	<i>Mesoaciditoga</i> ^{1,3}
Verrucomicrobia	0	0	0	10	<i>Spartobacteria</i> ⁴

Unknown	4.2	9.4	55	60
---------	-----	-----	----	----

590

591 However, subsequent PCR-primer development and confirmatory DNA sequencing
 592 successfully detected DNA signatures related to the fungal Trichocomaceae family
 593 (Ascomycota (division), Eurotiomycetes (class), and Eurotiales (order)) with
 594 *Talaromyces*, or related, DNA often showing closest resemblance. The following
 595 concentrations were found based on qPCR: 700.18 (approx. 10^2 gene copies/mg) and
 596 700.17 (approx. 10^1 gene copies/mg). 703.1, which appeared to have stronger DNA
 597 sequence bias towards *Aspergillus* sp. than *Talaromyces* sp., had approx. 10^3 gene
 598 copies/mg; signals in 703.2 were below detection (see suppl file 4).

599

600 To confirm the quality of PCR detection of the *Talaromyces* and related fungus
 601 products were sent for DNA sequencing (Eurofins Scientific) and compared via
 602 BLASTn algorithms to GenBank (National Centre for Biotechnology). All results were
 603 represented closely-related clades within the Eurotiale phylogenetic order, particularly:
 604 *Talaromyces*, *Penicillium* and *Aspergillus*. While it remains difficult to recognise
 605 specific microorganisms from short DNA sequence from a single locus, there were
 606 specific patterns in that could be discerned. Sample 700.17 showed the strongest
 607 evidences of specific *Talaromyces* species, with commonalities among the bi-
 608 directional reads, while the possibility for *Penicillium* sp. and *Aspergillus* sp. is still
 609 present. Sample 700.18 was clearly represented by either *Talaromyces* or *Penicillium*;
 610 both genera are teleomorphs, and *Talaromyces* sp. have historically been included
 611 within the *Penicillium* nomenclature; as such organisms in this clade may be mentioned
 612 in the literature interchangeably (Yilmaz et al., 2014; Frisvad, 2015), which further
 613 complicates recognition. Sample 703.1 showed greater alignments with *Aspergillus* and
 614 different *Penicillium* sp., and sample 703.2 had minimal DNA and had the least
 615 conclusive data (with greater mis-alignment of the sequences). It should be noted that
 616 the presence of a genus does not suggest antibiotic production, rather the possibility of
 617 micro-organisms that may produce exometabolites.

618

619 4. Discussion

620 4.1 Bioactivity - the contribution of the inorganic component (in reference to elements 621 Ti, Fe, Al and B as leachates or nanoparticles)

622

623 A total of 31 samples consisting of six archaeological medicinal clays (700.4, 700.17,
 624 700.18, 703.1, 703.2, 703.3), from Lemnos and Silesia, four natural Lemnos (700.19,
 625 700.20) and Melos clays (900.9, 933), eight synthetic clays (4,5,6,7,9,10,14,15)
 626 deriving from the spiking of two Melos natural clays with B, Al, Ti, Fe, two reference
 627 samples (SWy-2 and KGa-2) and their spiked with B, Al, Ti, Fe, counterparts (and
 628 three (non-clay) controls (3, 2, 8) were examined mineralogically, in bulk and for their
 629 nanoparticle composition, and chemically; they were all tested for bioactivity against
 630 *P aeruginosa* and *S aureus* following a method illustrated in the graphical abstract.

631

632 Of the above 31 samples, only 9 samples, a third, showed antibacterial activity against
 633 both Gram-positive and Gram-negative pathogens: archaeological samples 700.17,
 634 700.18 and synthetic samples 4 (Melos smectite spiked with B), 5 (Melos kaolinite
 635 spiked with B), and 7 (Melos kaolinite spiked with Al) as well as reference clays with
 636 both B and Al displayed antibacterial action.

637

638 For the purposes of this discussion we consider bioactive the samples which display
639 MIC₆₀ <50mg/ml. Reference clays, while not naturally bioactive, were rendered
640 bioactive with the addition of B and or Al. However the archaeological samples 700.17
641 and 700.18 did not contain sufficient concentrations of these two elements. Therefore
642 the question arises: why are these two samples bioactive? Before addressing this issue
643 we turn to a brief review of the literature regarding antimicrobial clays and the
644 mechanisms proposed, so far, for their antimicrobial activity.

645

646 Various researchers have attributed the bioactivity of the antimicrobial clays they have
647 investigated to different reasons: a) to the toxic influence of heavy metals such as Cu,
648 Zn and Ni (Otto et al., 2010); b) to the role of nanosized accessory Fe²⁺- bearing phases,
649 that might generate reactive oxygen species (Morrison et al. 2016; Williams 2017); c)
650 to the presence of soluble Al³⁺ (Londono et al., 2016); finally, d) to the existence of
651 Fe²⁺-atoms in active unsatisfied bonds at clay mineral edges which might form
652 hydroxide radicals upon oxidation (Wang et al., 2007). These studies have focused on
653 specific ions and heavy metals, but they did not necessarily offer definitive answers for
654 clay antimicrobial activity. For example, when these proposed mechanisms were
655 applied to clays other than those involved in the studies (for example Fe-saponite), they
656 yielded contradictory results (Zarate-Reyes et al., 2018).

657

658 Interestingly, none of the above studies has acknowledged or sought to investigate the
659 presence and contribution of an organic load. Indeed, all researchers have used clays
660 which have been sterilized in the autoclave, prior to any detailed investigation, thus
661 destroying any microorganisms within. Here we examine both the nature of the
662 microbiome and the contribution of each one of the elements already discussed in the
663 above studies i.e. Al, Fe, Ti and B; also the role of some transition metals in influencing
664 the bioactivity of the archaeological medicinal earths. Since the toxic influence of
665 transition metals has already been discussed (Otto et al., 2010; Otto & Heydel, 2013)
666 we note that, although largely present in the SE samples, these samples displayed low
667 or no bioactivity. Therefore we conclude that transition metals did not have a role to
668 play in driving the bioactivity of the two LEs.

669

670 *Titanium*

671 Recent work has shown that TiO₂ nanoparticles readily produce reactive oxygen species
672 (ROS) which are toxic to the membrane cells of bacteria, when exposed to visible light,
673 especially in arid environments (Georgiou et al., 2015). The generated ROS will be
674 rapidly converted to H₂O₂ upon contact with water by dismutation (i.e. simultaneous
675 oxidation and reduction) (Halliwell and Gutteridge, 2015). In this case, the antibacterial
676 activity will be controlled firstly by the abundance of TiO₂ reactive nanoparticles in the
677 leachate and secondly by the probability of contact and reaction between the generated
678 H₂O₂ and the bacterial cells. In the present study, although titanium is present in both
679 MEs and is considerably higher in SEs (Table 2). However, TiO₂ nanoparticles were
680 found primarily in 700.17 and 700.18, the bioactive LEs (Fig. 3) and not in the SEs
681 despite the presence of c.4% anatase (TiO₂ polymorph) in 703.2.

682 The two LE samples are indeed the more bioactive, thus corroborating the contribution
683 to bioactivity of TiO₂ nanoparticles rather than their ionic counterparts. Equally the
684 synthetic control samples of kaolinite and smectite (9 and 10) (Table 2) with 20%
685 anatase nanoparticles did not yield leachates with, as anticipated, antibacterial
686 properties. This may be due to aggregation of TiO₂ nanoparticles to larger particles,

687 which decreased their activity. Therefore, we suggest that the potential antibacterial
688 role of TiO₂ nanoparticles should be examined carefully. The formation of ROS as
689 mentioned above (Georgiou et al., 2015), would have necessitated a photochemical
690 reaction and therefore is not relevant to the present study. We conclude that the TiO₂
691 nanoparticles in 700.17 and 700.18 may play a small role in the samples' bioactivity
692 but their overall effect would depend on the amounts present.

693 *Fe-oxides*

694 The LE and the SE samples do not contain traceable amounts of Fe²⁺-bearing phases,
695 such as pyrite, which might have contributed to their antibacterial potential; this would
696 have taken place via generation of ROS, causing detrimental effect on bacteria through
697 oxidative stress, penetration of the cell wall and destruction of cellular components
698 (Cagnasso et al., 2010; Morrison et al., 2016; Williams, 2017). LEs 700.17 and 700.18
699 do contain Fe⁺ above the rest of the samples. However, the Fe-content of the
700 nanoparticles present in the leachates of the LEs is considerably lower than that of their
701 counterparts in the SEs, with the exception of 703.1; which showed low bioactivity.
702 When natural clays were spiked with Fe (oxides/ oxyhydroxides) hematite/goethite,
703 (samples 14, 15), they showed no bioactivity. We conclude that Fe⁺ in 700.17 and
704 700.18 might play a small role in the samples' bioactivity.

705 *Aluminium and Boron*

706 Aluminium originating from the dissolution of clay minerals and/or aluminium
707 sulphates in the leachates is toxic to cells and might trigger antibacterial action (e.g.
708 Londono et al., 2016; Williams, 2017). Similarly, boron has been reported to be
709 antibacterial (Photos-Jones et al., 2015). However, Al and B concentrations in the
710 leachates of 700.17 and 700.18 were very low compared to the rest of samples which
711 were not bioactive (Table 2). By contrast the Melos kaolinite spiked with alum (sample
712 7, Fig. 2) and especially the Melos alunogen (sample 3, Fig. 2) showed antibacterial
713 activity, particularly the latter. Melos kaolinite and smectite spiked with Boron are also
714 equally antibacterial (Fig. 2). We conclude that Al and B are not driving the bioactivity
715 of 700.17 and 700.18.

716

717 *Nanoparticle active edges*

718 The possible contribution of the active nanoparticle edges on the
719 antibacterial/bacteriostatic activity of the leachates should also be considered. All
720 leachates contain phyllosilicates, mainly illite, kaolinite and smectite along with anatase
721 and dolomite. Carbonates are not considered to have antibacterial properties and the
722 possible role of TiO₂-polymorphs such as anatase was considered previously.
723 Therefore, in this section we focus on the possible influence of the nanoparticle active
724 edges of clay minerals. Smectite edges have been shown to have oxidative capacity due
725 to formation of superoxide oxygen radical by chemisorption of oxygen atoms in
726 crystallite edges (Thompson and Moll, 1973), caused by simultaneous oxidation of
727 structural Fe²⁺, which have been shown to have antibacterial activity (Wang et al.,
728 2007).

729 The oxidative capacity of kaolinite and illite has not been evidenced so far. In the
730 present study the octahedral Fe in smectites is considered to be in Fe³⁺ form, which is
731 not known to contribute to bioactivity. However, the formation of superoxide oxygen
732 radicals in smectite edges might be controlled by particle size as well (Gournis et al.,

733 2002). In this aspect the smectite nanoparticles present in the leachates might also, to
734 some extent, contribute to the observed bioactivity of the LE samples. Nevertheless,
735 their importance should not be overemphasized. This because although illite, the main
736 phyllosilicate which might contain Fe²⁺, a potential source of superoxide oxygen
737 radicals nanoparticles, is present in both LE and SE earths, only the LE ones are
738 bioactive.

739 In conclusion, the clay nanoparticles present in the leachates of LE and SE samples do
740 not seem to be the dominant factors driving bioactivity. In the case of the synthetic
741 control samples bioactivity is controlled by the chemicals added, namely H₃BO₃ and
742 Al-sulfate and to a lesser degree by metals released such as Zn. The role of Fe²⁺-bearing
743 phases and active oxides such as TiO₂, which may produce superoxide oxygen radicals
744 during oxidation via Fenton-like reactions, seems also to be limited.

745

746 4.2 . Bioactivity – the contribution of the organic component

747 Most DNA signatures represented soil bacteria (Table 3); some species are recognised
748 as producers of antibacterial compounds. For example, *Bradyrhizobium* (alpha-
749 proteobacteria) found in bioactive 700.17 and 700.18 are bacteria commonly associated
750 with nitrogen-fixation in soils. They excrete porphyrins, which act as metal (M⁺²)
751 chelators and may become antibiotic precursors. 700.17 also contains abundant
752 *Achromobacter*, which are known hydrocarbon degraders that may produce
753 intermediary compounds with greater toxicity.

754

755 Further to the above, rhizobial bacteria, *Sphingomonas* and sulfur-related bacteria (e.g.
756 *Chlorobium*), naturally affect sulfur compounds which may increase solubility of
757 metals/metalloids potentially toxic to bacteria. However, since the concentrations of
758 these metals /metalloids in the SE and LE leachates (Table 3) are low, their contribution
759 to antibacterial activity must be considered to be limited. Moreover, *Pseudomonas*,
760 *Comamonadaceae*, *Arcobacteria*, *Aeromonas*, and *Achromobacter* contain species
761 related to pathogenesis although they may also be considered environmental. It is
762 concluded that both bioactive and non-bioactive MEs.

763

764 Apart from bacteria genetic analysis was also conducted on fungi (based on their
765 analogous 18S-rRNA gene). Of greatest interest was the presence, within samples
766 700.17 and 700.18, of Trichocomaceae (Eurotiales) fungi. Following genetic analysis
767 we discovered by in-silico analysis (via RDP and NCBI databases for genetic
768 sequences) that the “universal” primers for detecting fungus (e.g. Hadziavdic et al.,
769 2014), while able to capture many signatures for such communities, they would not
770 have recognized the 18S-rRNA from *Talaromyces*; as a result new genetic primers were
771 developed (see Methods section).

772

773 *Talaromyces* (and *Penicillium*) are saprotrophic organisms and contribute to the
774 spoilage of carbohydrate-rich foodstuff. But they are notorious producers of
775 exometabolites (Yilmaz et al., 2014; Frisvad, 2015), including antibiotics (e.g.
776 penicillin), and highly tolerant of extreme conditions (Samson, 2016). Both
777 *Talaromyces* are expected to form biofilms (on surface), when low on nutrients or
778 stressed, or be plankton-like (i.e., floating) when “feasting”. Being saprobes, living off
779 dead or decaying organic material, they will tend to remain at/near clay sediments; the
780 latter may help adsorb nutrients. They do not need light and will respire CO₂.

781

782 Another reason that the evidence for *Talaromyces* attracted our attention was the recent
783 publication by Pangging et al. (2019) who discovered that a new isolate, *Talaromyces*
784 *apiculatus* from Korean soil, produced bioanthracene. The detection of
785 bioanthracene has already been highlighted by Photos-Jones et al. (2017) and in
786 association with 700.18, the only one of the three LEs analysed at the time.

787

788 Although acknowledged, the specific mention of bioanthracene production by
789 *Talaromyces* remains, nevertheless, rather limited in literature (e.g. Yilmaz et al., 2014;
790 Pangling et al., 2019; Gao et al., 2013) with *T. apiculatus* being the one most
791 frequently mentioned. However, *Talaromyces* produce other bioactive compounds
792 summarized by Nicoletti and Trincone (2016) and Yilmaz et al., (2014) with beneficial
793 and detrimental health-related effects depending on exometabolite. Bioanthracene has
794 been found to be bioactive against the parasite *Plasmodium* and potentially against
795 bacteria as well (Saepua et al., 2018; Jaturapat et al., 2001).

796

797 Bioanthracene aside, *Talaromyces* sp. and some *Penicillium* sp. have also gained their
798 notoriety for their ability to produce polyketide-based pigments, many of which also
799 carry antibacterial properties (Caro et al., 2016; Rao et al., 2017). Conditions for their
800 production and excretion of exo-metabolites have been found to be environmentally
801 based, for example a source of carbohydrate, pH, temperature and geochemical
802 conditions in their surroundings (e.g. presence of potentially toxic elements, which
803 promote extra-cellular excretions) (Mendez et al., 2011; Santos-Ebinuma et al., 2013);
804 further, biotechnological efforts continue to research optimum production for the food
805 (e.g. Defosse, 2006) and textile industries as dye producers (Chadni et al., 2017).

806

807 5. Concluding remarks

808 Over the last few years we have been testing the bioactivity of archaeological medicinal
809 earths first, because it is a relatively straight forward parameter to measure, on the
810 grounds that they *might prove to be* useful antibacterials. Their historical use as
811 ‘antidotes to poison’ is too generic a description to begin to address experimentally and
812 in a meaningful way. This paper provides a quantitative assessment of the bioactivity
813 of six samples of medicinal earths from the collection of the Pharmacy Museum of the
814 University of Basel.

815

816 Of the six MEs only two LEs (700.17 and 700.18) are bioactive against specific *both*
817 Gram-positive and Gram-negative bacteria, while the third (700.4) is bioactive against
818 a Gram-positive only and a fourth, SE (703.1) is mildly antibacterial against Gram-
819 negative only. Bioactivity, under the conditions set out in this paper was defined as
820 having an MIC₆₀ < 50mg/ml.

821

822 The bioactivities of the leachates of 700.17 and 700.18 are comparable with synthetic
823 Melos smectite and kaolinite spiked with Boron and also Melos kaolinite spiked with
824 Al. There is good agreement between the Melos and the reference smectites and kaolins
825 in that although the latter are not naturally antibacterial, they become antibacterial when
826 spiked with Al and B. We have noted that 700.17 and 700.18 are Al and B deficient
827 and so they cannot be bioactive on account of these two elements.

828

829 Looking at other reasons for their bioactivity and more specifically into their
830 microbiomical load, we note that 700.17 and 700.18 contain, with certainty, the fungus
831 *Talaromyces* spp. A greater certainty for the fungus *Aspergillus* (another member of

832 the phylogenetic clade) and a different *Penicillium* were suggested for 703.1 which was
833 mildly antibacterial against *P. aeruginosa*, only. We conclude that the fungal, rather
834 than the bacterial load, is the key driver imparting bioactivity to the three MEs
835 examined here (700.17, 700.18 and to a lesser extent in 703.1)

836

837 Based on a protocol of analysis (illustrated in the graphic abstract), we suggest that
838 antibacterial activity of archaeological MEs seems to derive primarily from the clays'
839 organic load; the contribution of TiO₂ nanoparticles, if in sufficient numbers might
840 have also a role to play. We do not know how the LEs examined here acquired their
841 specific organic load. We acknowledge that *Talaromyces* and *Penicillium* are
842 ubiquitous but they have not been found to be present in the Lemnos natural clays
843 examined here and neither were the latter shown to be antibacterial, being deficient in
844 both key elements (A1 and B) as well as relevant organic load. We conclude that clays
845 with a fungal and/or bacterial load might be worth investigating further as potentially
846 serious antibacterial agents.

847

848

849 **Acknowledgements**

850 The authors are indebted to Mrs Corinne Eichenberger and the director and Trustees
851 of the Pharmacy Museum of the University of Basel for making the archaeological
852 samples available for analysis. Also Ms N Andriopoulou, University of Crete, for the
853 preparation of synthetic clays and the unknown reviewers for their constructive queries
854 and comments.

855

856

857 **Funding**

858 Funding has been provided by: Wellcome Trust (Seed Award in the Humanities and
859 Social Sciences (201676/Z/16/Z); and NERC-FENAC award (FENAC/2015/11/07).

860 The work is part of a larger study into Greco–Roman antimicrobial minerals. Principal
861 investigator: E. Photos-Jones.

862

863

864 **Authors' contributions**

865 GEC- responsible for mineralogical /elemental analysis and interpretation, author of
866 relevant sections.

867 CK- responsible for DNA sequencing and interpretation of ME microbiome, author of
868 relevant sections.

869 DV and IG - responsible for MIC measurements, interpretation of antibacterial activity
870 and authorship of relevant section.

871 CE and EVJ- responsible for nanoparticle analysis, interpretation and authorship of
872 relevant section.

873 EPJ - initiator/coordinator of project and responsible for overall preparation and
874 manuscript submission and resubmission after reviewing.

875

876

877

878 **References**

879

880 Andrews J.M., 2001. Determination of minimum inhibitory concentrations. J.
881 Antimicrob. Chemother. 48, Suppl.S1, 5-16.

882
883 Anderson, J.U., 1963. An improved pretreatment for mineralogical analysis of
884 samples containing organic matter. *Clays and Clay Minerals* 10, 380--387.
885
886 Brock, A.J., 1929. *Greek medicine being extracts illustrative of medical writers from*
887 *Hippocrates to Galen.* Dent, London.
888
889 Cagnasso, M., Boero, V., Franchini, M.A., Chorover, J., 2010. ATR-FTIR studies of
890 phospholipid vesicle interactions with α -FeOOH and α -Fe₂O₃ surfaces. *Colloids*
891 *Surfaces B. Biointerfaces* 76, 456–467. [https://doi: 10.1016/j.colsurfb.2009.12.005](https://doi.org/10.1016/j.colsurfb.2009.12.005).
892
893 Caro, Y., Venkatachalam, M., Lebeau, J., Fouillaud, M., Defosse, L., 2016.
894 Pigments and colorants from filamentous fungi, in: Merillon, J-M., Ramawat, K.G.
895 (Eds.), *Fungal Metabolites, Reference Series in Phytochemistry.* Switzerland,
896 Springer International Publishing. [https://doi 10.1007/978-3-319-25001-4_26](https://doi.org/10.1007/978-3-319-25001-4_26).
897
898 Chadni, Z., Rahaman, M.H., Jerin, I., Hoque, K.M.F., Reza, M.A., 2017. Extraction
899 and optimisation of red pigment production as secondary metabolites from
900 *Talaromyces verruculosus* and its potential use in textile industries. *J. Fungal Biol.*
901 8(1), 48-57.
902
903 Cole, J.R., Wang, Q., Fish, J.A., Chai, B., McGarrell, D.M., Sun, Y., Brown, C.T.,
904 Porras-Alfaro, A., Kuske, C.R., Tiedje, J.M., 2014. Ribosomal Database Project: data
905 and tools for high throughput rRNA analysis. *Nucl. Acids Res.* 42(Database issue):
906 D633-D642; [https://doi: 10.1093/nar/gkt1244](https://doi.org/10.1093/nar/gkt1244).
907
908 Defosse, L., 2006. Microbial production of food grade pigments. *Food Technol.*
909 *Biotechnol.* 44, 313-21.
910
911 Dannenfeldt, K.H., 1984. The introduction of a new sixteenth century drug: Terra
912 Silesiaca. *Medical History* 28, 174-188.

913 Duffin, C.J., 2013. Some early eighteenth century geological *Materia Medica.* In
914 Duffin, C. J., Moody, R. T. J. & Gardner-Thorpe, C. (eds) 2013. *A History of*
915 *Geology and Medicine.* Geological Society, London, Special Publications, **375**,209-
916 233.

917 Frisvad, J.C., 2015. Taxonomy, chemodiversity, and chemoconsistency of
918 *Aspergillus*, *Penicillium* and *Talaromyces* species. *Front. Microbiol.* 12. [https://doi](https://doi.org/10.3389/fmicb.2014.00773)
919 [10.3389/fmicb.2014.00773](https://doi.org/10.3389/fmicb.2014.00773).
920
921 Gao, H., Zhou, L., Li, D., Gu, Q., Zhu, T.J., 2013. New cytotoxic metabolites from
922 the marine-derived fungus *Penicillium* sp. ZLN29. *Helv. Chim. Acta* 96, 51-19.
923
924 Georgiou, C.D., Sun, H., McKay, C.P., Grintzalis, K., Papapostolou, I., Zisimopoulos,
925 D., Zhang, G., Koutsopoulou, E., Christidis G. and Margiolaki, I., 2015. Detection of
926 photochemical superoxide radicals in chemically reactive desert soils. *Nature*
927 *Communications.* [https:// doi 10.1038/ncomms8100](https://doi.org/10.1038/ncomms8100).
928

- 929 Gournis, D., Karakassides, M.A., Petrides, D., 2002. Formation of hydroxyl radicals
930 catalyzed by clay surfaces. *Physics and Chemistry of Minerals* 29, 155-158.
931
- 932 Hall, A.J., Photos-Jones, E. 2008. Accessing past beliefs and practices: the case of
933 Lemnian Earth. *Archaeometry* 50, 1034–1049.
934
- 935 Halliwell, B., Gutteridge, C.M.J., 2015. *Free Radicals in Biology and Medicine* 3rd
936 ed.. Oxford, Oxford University Press.
937
- 938 Hadziavdic, K., Lekang K., Jonassen, I., Thompson, E.M., Troedsson, C., 2014.
939 Characterization of the 18S rRNA Gene for Designing Universal Eukaryote Specific
940 Primer. *PLOS*. <https://doi.org/10.1371/journal.pone.0087624>.
- 941
- 942 Hardy, A., Rollinson, G., 2016. A chemical study of a 'Terra Sigillata' medicinal tablet
943 from a late 17th century Italian medicine chest. *Pharmaceutical Historian* 46(1), 2-7.
944
945
- 946 Hasluck, F.W., 1909–1910. Terra Lemnia. *Annual British School at Athens* XVI,
947 220–231.
948
- 949 Hasluck, F.W., Hasluck, M.M., 1929. *Christianity and Islam under the Sultans. Terra*
950 *Lemnia, II*, Oxford, Clarendon Press.
951
- 952 Haydel S.E., Remenih C.M., Williams L.B., 2008. Broad-spectrum in vitro
953 antibacterial activities of clay minerals against antibiotic-susceptible and
954 antibiotic-resistant bacterial pathogens. *J Antimicrob Chemother* 61:353–361 .
955 doi: 10.1093/jac/dkm468
956
- 957 Jaturapat, A., Isaka, M., Hywel-Jones, N.L., Lertwerawat, Y., Kamchonwongpaisan,
958 S., Kirtikara, K., Tanticharoen, M., Thebtaranonth, Y., 2001. Bioanthracenes from
959 the insect pathogenic fungus *Cordyceps pseudomilitaris* BCC1620. I. Taxonomy,
960 fermentation, isolate, and antimalarial activity. *J. Antibiot.* 54, 29-35.
961
- 962 Keller, N.P., 2019. Fungal secondary metabolism: regulation, function and drug
963 discovery. *Nature Rev. Microbiol.* 17, 167-180.
964
- 965 Knapp, C.W., Graham, D.W., 2004. Development of alternate ssh-rRNA probing
966 strategies for characterizing aquatic communities. *J. Microbiol. Meth.* 56(3), 323-
967 330. <https://doi: 10.1016/j.mimet.2003.10.017>.
968
- 969 Locatelli, F.M., Goo, K-S., Ulanova, U., 2016. Effects of trace metal ions on
970 secondary metabolism and the morphological development of streptomycetes.
971 *Metallomics* 8, 469. <https://doi 10.1039/c5mt00324e>.
972
- 973 Londono, S.C., Hartnett, H.E., Williams, L.B., 2016. Unraveling the antibacterial mode
974 of action of a clay from the Colombian Amazon. *Environ. Geochem. Health* 38, 363–
975 379. <https://doi: 10.1007/s10653-015-9723-y>.
976
- 977 MacGregor, A., 2013. Medicinal terra sigillata: a historical, geographical and

978 typological review, in: Duffin, C.J., Moody, R.T.J., Gardner-Thorpe, C. (Eds.), A
979 History of Geology and Medicine. London, Geological Society, Special Publications
980 375, 113–136, <https://doi.org/10.1144/SP375.29>.
981

982 Macheleidt, J., Mattern, D.J., Fischer, I., Netzker, T., Weber, I., Schroeckh, V.,
983 Valiante, V., Brakhage, A.A., 2016. Regulation and role of fungal secondary
984 metabolites. *Ann. Rev. Genetics* 50, 371-392.
985

986 Manaia C.M., Macedo, G., Fatta-Kassinos, D., Nunes, O.,C., 2016. Antibiotic
987 resistance in urban aquatic environments: can it be controlled? *Appl Microbiol*
988 *Biotechnol* 100:1543–1557 . doi: 10.1007/s00253-015-7202-0
989

990 Maidak B.L., Cole, J.R., Lilburn, T.G., Parker, C.T., Saxman, R., Farris, R.J., Garrity,
991 G.M., Olsen, G.L., Schmidt, T.M., Tiedje, T.G., 2001, The RDP-II (Ribosomal
992 Database Project). *Nucl Acid Rs* 29(1): 173
993

994 Medina, A., Schmidt-Heydt, M., Rodríguez, A., Parra, R., Geisen, R., Magan, N.,
995 2015. Impacts of environmental stress on growth, secondary metabolite biosynthetic
996 gene clusters and metabolite production of xerotolerant/xerophilic fungi. *Current*
997 *Genetics* 61(3), 325-34. <https://doi: 10.1007/s00294-014-0455-9>.
998

999 Mendez, A., Perez, C., Montanez, J.C., Martinez, G., Aguilar, C.N., 2011. Red
1000 pigment production by *Penicillium purpurogenum* GH2 is influenced by pH and
1001 temperature. *Biomed. Biotechnol.* 12, 961-8.
1002

1003 Morrison, K.D., Misra, R., Williams, L.B., 2016. Unearthing the Antibacterial
1004 Mechanism of Medicinal Clay: A Geochemical Approach to Combating Antibiotic
1005 Resistance *Scientific Reports*, DOI: 10.1038/srep19043
1006

1007 Nicoletti, R., Trincone, A., 2016. Bioactive compounds produced by strains of
1008 *Penicillium* and *Talaromyces* of marine origin. *Mar. Drugs* 14: 37
1009

1010• Nutton, V., 2004. *Ancient Medicine*. London ; New York : Routledge
1011

1012 Otto, C.C., Cunningham, T.M., Hansen, M.R., Haydel, S.E., 2010. Effects of
1013 antibacterial mineral leachates on the cellular ultrastructure, morphology, and
1014 membrane integrity of *Escherichia coli* and methicillin-resistant *Staphylococcus*
1015 *aureus*. *Ann. Clin. Microbiol. Antimicrob.* 9:26. doi: 10.1186/1476-0711-9-26.
1016

1017 Otto, C.C., Haydel, S.E., 2013. Exchangeable Ions Are Responsible for the In Vitro
1018 Antibacterial Properties of Natural Clay Mixtures. *PLoS One* 8, 1–9. [https:// doi: 10.1371/journal.pone.0064068](https://doi: 10.1371/journal.pone.0064068).
1019

1020

1021 Pettit, R.K., 2011. Small-molecule elicitation of microbial secondary metabolites,
1022 *Microb. Biotechnol.* 4(4), 471-8. <https://doi: 10.1111/j.1751-7915.2010.00196.x>.
1023

1024 Photos-Jones, E. , Keane, C., Jones, A.X., Stamatakis, M., Robertson, P., Hall,
1025 A.J., Leanord, A., 2015. Testing *Dioscorides'* medicinal clays for their antibacterial
1026 properties: the case of Samian Earth. *J. Arch. Sci.* 57, 257-
1027 267. (doi:10.1016/j.jas.2015.01.020)

1028
1029 Photos-Jones, E. , Christidis, G.E., Piochi, M., Keane, C., Mormone, A., Balassone,
1030 G., Perdikatsis, V. and Leanord, A., 2016. Testing Greco-Roman medicinal minerals:
1031 The case of solfataric alum. *Journal of Archaeological Science: Reports*, 10, pp. 82-
1032 95. (doi:10.1016/j.jasrep.2016.08.042)
1033
1034 Photos-Jones, E., Edwards, C., Häner, F., et al., 2017. Archaeological medicinal earths
1035 as antibacterial agents: the case of the Basel Lemnian sphragides. London, Geological
1036 Society, Special Publications 452. [https:// doi: 10.1144/SP452.6](https://doi.org/10.1144/SP452.6).
1037
1038 Photos-Jones, E., Knapp, C.W., Venieri, D., Christidis, G.E., Elgy, C., Valsami-Jones,
1039 E., Gounaki, I., Andriopoulou, N.C., 2018. Greco-Roman mineral (litho)therapeutics
1040 and their relationship to their microbiome: The case of the red pigment *miltos*. *J.*
1041 *Arch. Sci. Rep.* 22(12), 179-192. <https://doi.org/10.1016/j.jasrep.2018.07.017>.
1042
1043 Photos-Jones, E., Hall, A.J., 2011. Lemnian Earth and the Earths of the Aegean: an
1044 Archaeological Guide to Medicines, Pigments and Washing Powders. Glasgow,
1045 Pottingair Press.
1046
1047 Rao, M.P.N, Xiao, M., Li, W-J., 2017. Fungal and bacterial pigments: secondary
1048 metabolites with wide applications. *Front. Microbiol.* 8, 1113.
1049
1050 Samson, R.A., 2016. Cellular constitution, water and nutritional needs, and secondary
1051 metabolites, in: *ADD EDS : Environmental Mycology in Public Health*. Elsevier.
1052 [https://doi 10.1016/B978-0-012.411471-5.000001-6](https://doi.org/10.1016/B978-0-012-411471-5.000001-6).
1053
1054 Saepua, S., Kornsakulkarn, J., Somyong, W., Laksanacharoen, P., Isaka, M., 2018.
1055 Bioactive compounds from the scale insect fungus *Conoideocrella tenuis* BCC 44534.
1056 *Tetrahedron* 74, 859-866.
1057
1058 Swetha S, Santhosh S.M., Balakrishna R.G., 2010. Enhanced bactericidal activity of
1059 modified titania in sunlight against pseudomonas aeruginosa, a water-borne
1060 pathogen. *Photochem Photobiol* 86:1127–1134 . doi: 10.1111/j.1751-
1061 1097.2010.00781.x
1062
1063 Santos-Ebinuma, V.C., Teixeira, M.F.S., Pessoa Jr., A., 2013. Submerged culture
1064 conditions for the production of alternative natural colorants by a new isolated
1065 *Penicillium purpurogenum* DPUA 1275. *J. Microbiol. Biotechnol.* 23, 802-810.
1066
1067 Sealy, F.L.W., 1919. Lemnos. *Annual British School at Athens* 22, 164–165.
1068
1069 Tourptsoglou-Stephanidou, B., 1986. Ταξιδιωτικά και γεωγραφικά κείμενα για την
1070 νήσο Λήμνο (15-20 αιώνας) (Geographic and Travellers' accounts for the island of
Lemnos (15th-20th century). University of Thessaloniki, Polytechnic School IX, Suppl
33.
1071
1072 Tyc, O., Song, C., Dickschat, J.S., Vos, M., Garbeva, P., 2016. Ecological role of
1073 volatile and soluble secondary metabolites produced by soil bacteria. *Trends in*
1074 *Microbiology* 25(4), 280-92. [https://doi: 10.1016/j.tim.2016.12.002](https://doi.org/10.1016/j.tim.2016.12.002)

1075 Wang, Q., Garrity, G.M., Tiedje, J.M. Cole, J.R., 2007. Naïve Bayesian Classifier for
1076 Rapid Assignment of rRNA Sequences into the New Bacterial Taxonomy. *Appl.*
1077 *Environ. Microbiol.* 73(16), 5261-5267. [https:// doi: 10.1128/AEM.00062-07](https://doi.org/10.1128/AEM.00062-07).
1078
1079 Venieri D., Gounaki I., Bikouvaraki M., Binas V., Zachopoulos A., Kiriakidis G.,
1080 Mantzavinos D., 2017a. Solar photocatalysis as disinfection technique:
1081 Inactivation of *Klebsiella pneumoniae* in sewage and investigation of changes in
1082 antibiotic resistance profile. *J Environ Manage* 195: . doi:
1083 10.1016/j.jenvman.2016.06.009
1084
1085 Venieri D., Tournas F., Gounaki I., Binas V., Zachopoulos A., Kiriakidis G.,
1086 Mantzavinos D., 2017b. Inactivation of *Staphylococcus aureus* in water by
1087 means of solar photocatalysis using metal doped TiO₂ semiconductors. *J Chem*
1088 *Technol Biotechnol* 92:43–51 . doi: 10.1002/jctb.5085
1089
1090
1091 Williams, L.B., 2017. Geomimicry: harnessing the antibacterial action of clays. *Clay*
1092 *Miner.* 52, 1-24.
1093
1094 Yilmaz, N., Visagie, C.M., Houbraeken, J., Frisvad, J.C., Samson, R.A.,
1095 2014. Polyphasic taxonomy of genus *Talaromyces*. *Stud. Mycology* 78, 175-341.
1096
1097 Zarate-Reyes, L., Lopez-Pacheco, C., Nieto-Camacho, A., Palacios, E., Gómez-
1098 Vidales, V., Kaufhold, S., Ufer, C., García Zepeda, E., Cervini-Silva, J., 2018.
1099 Antibacterial clay against Gram-negative antibiotic resistant bacteria. *J. Hazardous*
1100 *Materials* 342, 625-632.
1101
1102